Journal of Coordination Chemistry

ISSN: 0095-8972 (Print) 1029-0389 (Online) Journal homepage: http://www.tandfonline.com/loi/gcoo20

Copper tetradentate N_2Py_2 complexes with pendant bases in the secondary coordination sphere: improved ligand synthesis and protonation studies

Juliet F. Khosrowabadi Kotyk, Joseph W. Ziller & Jenny Y. Yang

To cite this article: Juliet F. Khosrowabadi Kotyk, Joseph W. Ziller & Jenny Y. Yang (2016) Copper tetradentate N_2Py_2 complexes with pendant bases in the secondary coordination sphere: improved ligand synthesis and protonation studies, Journal of Coordination Chemistry, 69:11-13, 1990-2002, DOI: 10.1080/00958972.2015.1130223

To link to this article: http://dx.doi.org/10.1080/00958972.2015.1130223

JOURNAL OF COORDINATION CHEMISTRY, 2015
VOL. 69, NOS. 11–13, 1990–2002
http://dx.doi.org/10.1080/00958972.2015.1130223

Taylor & Francis
Taylor & Francis Group

Copper tetradentate N_2Py_2 complexes with pendant bases in the secondary coordination sphere: improved ligand synthesis and protonation studies

Juliet F. Khosrowabadi Kotyk, Joseph W. Ziller and Jenny Y. Yang

Department of Chemistry, University of California, Irvine, CA, USA

ABSTRACT

An improved preparation for a tetradentate neutral N_2Py_2 ligand with two dimethylamine functionalities in the secondary coordination sphere ($\mathbf{L^{DMA}}$) is reported. This synthetic route uses cheaper and more readily available precursors with fewer steps and greater overall yield. The synthesis and characterization of the corresponding Cu(II) and Cu(I) complexes of this ligand and its analog lacking pendant bases ($\mathbf{L^{H}}$) are also described. The cyclic voltammograms indicate that the Cu(II/I) couple for the $\mathbf{L^{DMA}}$ complex is over 400 mV positive of the quasi-reversible Cu(II/I) couple for the L^{H} complex. Structural characterization indicates this is likely a result of steric effects in $[Cu(L^{DMA})]^{2+}$ that are not present in the $[Cu(L^{H})]^{2+}$ complex. Protonation of both diamagnetic Cu(I) complexes is cleanly reversible. ^{1}H NMR spectroscopic studies of the protonated complexes reveals that protonation occurs on the tertiary amines in the ligand backbone for both complexes.

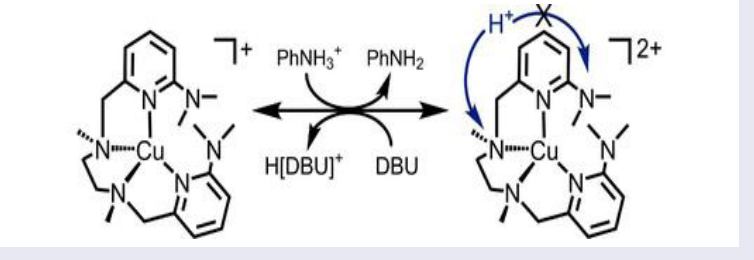

ARTICLE HISTORY
Received 15 September 2015
Accepted 23 October 2015

KEYWORDS
Copper complex; protonation; cyclic voltammetry; pendant base; secondary coordination sphere; N_2Py_2

1. Introduction

Proton relays play an essential role in mediating redox reactivity in biological and synthetic systems. Enzymes incorporate distal proton donors and acceptors to preorganize metalloenzyme active sites for catalysis and facilitate proton-coupled electron transfer [1–5]. In order to mimic this environment in transition metal complexes, many new ligands have been developed that incorporate functionalities to manage proton inventory in the secondary coordination sphere [6-28]. The resulting complexes often display more selective, efficient, or rapid catalysis than analogs that lack proton relays [29–52].

CONTACT Jenny Y. Yang j.yang@uci.edu
Supplemental data for this article can be accessed at http://dx.doi.org/10.1080/00958972.2015.1130223.

Neutral tetradentate diamino–dipyridal ligands (N_2Py_2) have commonly been used as a scaffold for transition metal-mediated catalysis in a variety of different reactions, including olefin epoxidation [53–58] and alkane [59–65], alcohol [66], and water oxidation [67]. We previously reported the synthesis of a modified N_2Py_2 with dimethylamine pendant bases installed at the 2-positions of the pyridine rings in order to study the effect of secondary coordination sphere proton acceptors on oxidative catalysis ($\mathbf{L^{DMA}}$) [28]. This ligand preparation required multiple steps and the use of an expensive starting material. To facilitate additional studies with this ligand, we report herein a vastly improved two-step preparation using cheaper and more accessible precursors to furnish the ligand in higher yield. In order to investigate the effect of the pendant bases, the congener without pendant bases ($\mathbf{L^{H}}$) was also synthesized, shown in Chart 1.

Although amines are generally used as Brönsted bases, protonated pendant bases can also serve as effective proton donors to coordinated substrates [39, 68–70]. In an effort to study the single protonation of these ligands in a transition metal complex and the pK_a of the resulting acid, the Cu(I) complexes (**3** and **4**) were prepared and structurally characterized from their respective Cu(II) complexes (**1** and **2**). The protonation of the diamagnetic Cu(I) complexes could then be easily investigated using ^{1}H NMR spectroscopy.

2. Results and discussion

2.1. Synthesis of ligands L^H and L^{DMA}

The synthesis of $\mathbf{L^{H}}$, which contains no pendant base functionalities, has been previously reported [71]. As shown in Scheme 1 (top), nucleophilic substitution under basic conditions using N,N′-dimethylethylenediamine and 2-(chloromethyl)pyridine provides $\mathbf{L^{H}}$ in 91% yield.

The synthesis of $\mathbf{L^{DMA}}$, which incorporates two dimethyl amine (DMA) functionalities in the secondary coordination sphere, has also been reported previously [28]. However, the prior procedure required the expensive and not readily available precursor 6-(dimethylamino)picolinaldehyde. We independently prepared the precursor in three steps using a published procedure [72] (64% yield) to deliver the ligand in 33% yield overall.

In order to facilitate our ligand preparation, we developed an improved route to $\mathbf{L^{DMA}}$ (shown in Scheme 1, bottom). One-pot reductive amination using N,N′-dimethylethylenediamine and 6-bromo-2-formylpyridine followed by deprotonation yields the N_2Py_2 ligand containing bromo- functionalities in the 6- and 6′ positions [57]. Nucleophilic aromatic substitution using aqueous dimethylamine under pressure affords $\mathbf{L^{DMA}}$ [73]. This preparation uses inexpensive and more readily available reagents. In addition, the yield is increased to 85%, offering significant improvements over the previously published synthesis.

2.2. Synthesis, characterization, and single-crystal X-ray diffraction studies on copper complexes

Both $[CuL^{H}][BF_4]_2$ (**1**) and $[CuL^{DMA}][BF_4]_2$ (**2**) were synthesized by adding one equivalent of solid $[Cu(CH_3CN)_4][BF_4]_2$ to the respective ligand solutions and stirring for 0.5 h at room temperature. Complex **1** was isolated by addition of diethyl ether followed by trituration of the blue oil with toluene to precipitate a dark blue powder in quantitative yield. Complex **2** was isolated by precipitation from diethyl ether to isolate a dark purple powder in 82% yield. The formulation and purity, respectively, of **1** and **2** were confirmed by ESI-MS and elemental analysis.

Single crystals of $[CuL^{H}][BF_4]_2$ (**1**) were grown by the evaporation of acetonitrile from a 50 : 50 mixture of acetonitrile/toluene to give dark blue crystals that were analyzed by X-ray diffraction. In addition to $\mathbf{L^{H}}$, the copper center has an acetonitrile bound to give a five-coordinate coordination environment. The methyl groups on the amine backbone are *cis* to one another. The coordination geometry can be described as pseudo square pyramidal with a τ_5 value of 0.36, where $\tau_5 = 1$ is an ideal trigonal bipyramidal

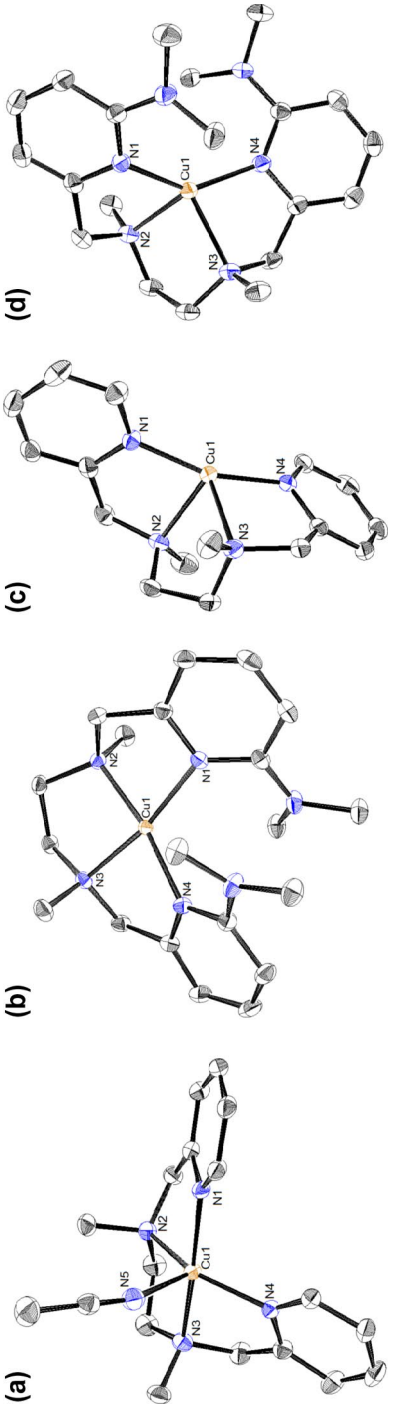

Figure 1. ORTEP diagrams of (a) $[CuL^{H}][BF_4]_2$ (**1**), (b) $[CuL^{DMA}][BF_4]_2$ (**2**), (c) $[CuL^{H}][BF_4]$ (**3**), and (d) $[CuL^{DMA}][BF_4]$ (**4**). Thermal ellipsoids are drawn at 50% probability. Hydrogens and BF_4 anions are omitted for clarity.

Table 1. Selected bond distances in crystal structures. N(1) and N(4) are pyridine nitrogens and N(2) and N(3) are backbone amine nitrogen. Bond distances are given in angstroms.

Bond	$[CuL^{H}][BF_4]_2$	$[CuL^{DMA}][BF_4]_2$	$[CuL^{H}][BF_4]$	$[CuL^{DMA}][BF_4]$
Cu–N1	2.0000(16)	1.9777(11)	1.943(2)	2.0216(12)
Cu–N2	2.0180(17)	1.9915(11)	2.219(2)	2.1723(13)
Cu–N3	2.0383(17)	1.9777(11)	2.217(2)	2.1791(12)
Cu–N4	2.0109(17)	1.9915(11)	1.945(2)	2.0184(12)

and $\tau_5 = 0$ is an ideal square pyramidal geometry [74]. Single crystals of $[CuL^{DMA}][BF_4]_2$ (**2**) were grown by the vapor diffusion of diethyl ether into an acetonitrile solution to give dark purple crystals. In contrast to $[CuL^{H}][BF_4]_2$ (**1**), the X-ray crystal structure of $[CuL^{DMA}][BF_4]_2$ (**2**) is four coordinate with a mildly distorted square planar geometry and a τ_4 value of 0.15, where $\tau_4 = 1$ is an ideal tetrahedral and $\tau_4 = 0$ is an ideal square planar geometry [75]. The two methyl groups on the amine backbone are *trans* to one another while the dimethylamine functionalities are stacked directly above one another. The structures for **1** and **2** are shown in Figure 1(a) and (b), respectively, with selected bond distances in Table 1.

The Cu(I) species, $[CuL^{H}][BF_4]$ (**3**) and $[CuL^{DMA}][BF_4]$ (**4**), were synthesized by chemical reduction with one equivalent of potassium graphite. After a color change from dark blue to yellow and dark purple to yellow, respectively, the solution was filtered and the solvent was removed to give the monovalent **3** and **4**. This was successful with both complexes and the resulting diamagnetic complexes were characterized by ^{1}H NMR spectroscopy (Figures S1 and S2, Supporting Information), ESI-MS and elemental analysis. Both $[CuL^{H}][BF_4]$ (**3**) and $[CuL^{DMA}][BF_4]$ (**4**) are air stable.

Single crystals of $[CuL^{H}][BF_4]$ (**3**) were grown by vapor diffusion of diethyl ether into an acetonitrile solution to give yellow crystals. The X-ray crystal structure is shown in Figure 1(c) and selected bond distances in Table 1. The solid-state structure exhibits a pseudotetrahedral geometry ($\tau_4 = 0.52$). The methyl groups in the amine backbone are *trans* to each other in contrast to the divalent complex. Single crystals were grown of $[CuL^{DMA}][BF_4]$ (**4**) by room temperature evaporation of a dichloromethane solution to give light yellow crystals. The X-ray crystal structure is shown in Figure 1(d), with selected bond distances in Table 1 ($\tau_4 = 0.64$). The methyl groups in the amine backbone are *trans* to each other. Both monovalent copper structures **3** and **4** are in a distorted tetrahedral geometry consistent with a Cu(I) d^{10} metal ion.

2.3. Electrochemical studies

The cyclic voltammograms of $\mathbf{L^H}$ and $\mathbf{L^{DMA}}$ are shown in Figures S3 and S4 in the Supporting Information. The cyclic voltammograms of $[CuL^{H}][BF_4]_2$ (**1**) exhibited a quasi-reversible event at $E^{o\prime} = -0.48$ V (at 100 mV/s, $i_a/i_c = 0.65$, $\Delta E_p = 121$ mV compared to $\Delta E_p = 59$ mV for $FeCp_2^{0/+}$) attributed to the Cu(II/I) couple. The scan rate dependence is shown in Figure 2 and the parameters are listed in Table S1 in the Supporting Information. ΔE_p increases with scan rate as expected for a quasi-reversible redox event, indicating that the rate of electron transfer is slow and on the same order of magnitude as mass transport. The five-coordinate complex likely dissociates the acetonitrile ligand upon reduction to Cu(I), which may also contribute to the quasi-reversible nature of this couple. An irreversible reduction event (see Figure S5 in Supporting Information) was observed at $E_{pc} = -2.26$ V, which remained completely irreversible at the scan rates examined (25–1600 mV s^{-1}).

Cyclic voltammetry of $[CuL^{DMA}][BF_4]_2$ (**2**) at 100 mV s^{-1} also displayed two reduction events. Cyclic voltammetry of $[CuL^{H}][BF_4]_2$ (**1**) has a reversible event at $E_{1/2} = -0.058$ V (at 100 mV s^{-1}, $i_a/i_c = 0.91$, $\Delta E_p = 114$ mV compared to $\Delta E_p = 106$ mV for $FeCp_2^{0/+}$) attributed to the Cu(II/I) couple, shown in Figure 3. The changes in anodic and cathodic currents by scan rate indicated diffusion control behavior by the complex (see Table S2 in the Supporting Information). An irreversible reduction event observed at $E_{pc} = -1.77$ V remained irreversible at the scan rates examined (25–1600 mV s^{-1}).

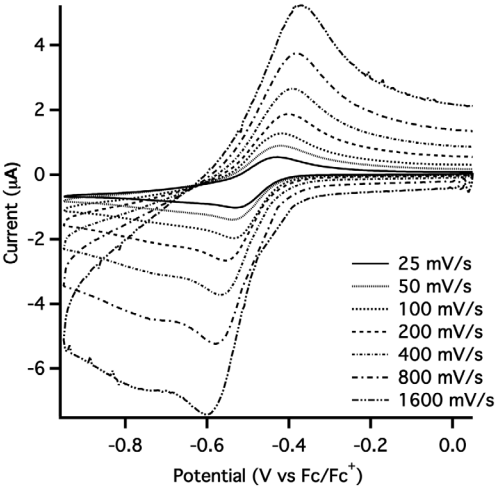

Figure 2. Scan rate-dependent cyclic voltammogram of Cu(II/I) couple in 1.0 mM $[CuL^{H}][BF_4]_2$ (**1**) in a solution containing 0.10 M Bu_4NBF_4 in CH_3CN.

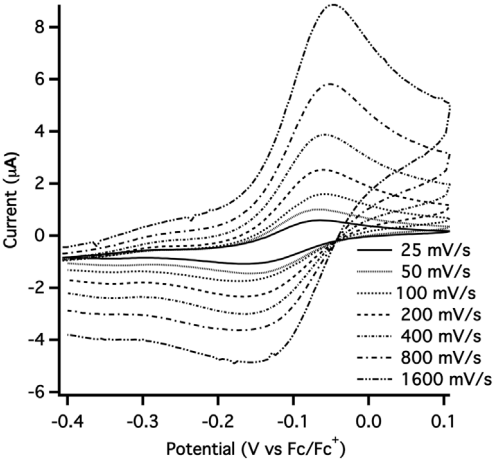

Figure 3. Scan rate dependent cyclic voltammogram of Cu(II/I) couple in 1.0 mM $[CuL^{DMA}][BF_4]_2$ (**2**) in a solution containing 0.10 M Bu_4NBF_4 in CH_3CN.

The Cu(II/I) couple is observed at a significantly more positive potential for CuL^{DMA} versus CuL^{H}. The one electron reduction of d^9-Cu(II) to d^{10}-Cu(I) is accompanied by a geometric rearrangement to tetrahedral from a pseudo-square pyramidal in $[CuL^{H}(CH_3CN)]^{2+}$ or square planar geometry in $[CuL^{DMA}]^{2+}$. It is likely that releasing the steric strain from the nearly coplanar dimethylamine functionalities in $[CuL^{DMA}]^{2+}$ by reduction to the corresponding tetrahedral complex contributes to the positive reduction potential compared to $[CuL^{H}(CH_3CN)]^{2+}$, which is not sterically strained. This steric effect on the Cu(II/I) redox potential has been observed in other tetradentate copper complexes [76].

2.4. Protonation studies

In an effort to guage the pK_a of the pendant bases of the copper complex, protonation studies of diamagnetic $[CuL^{DMA}][BF_4]$ (**4**) were investigated using ^{1}H NMR spectroscopy, shown in Figure 4. Addition

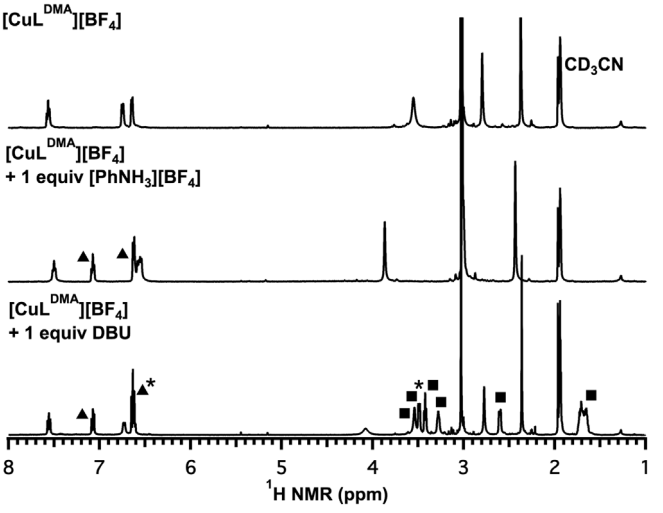

Figure 4. ^{1}H NMR spectra of [CuL^{DMA}][BF$_4$] (**4**) in the presence of acid and base. Top: complex with no acid or base present. Middle: 1 equiv [PhNH$_3$][BF$_4$] added, triangle symbol (▲) indicates aniline resonances. Bottom: 1 equiv DBU added, square symbol (n) indicates [HDBU][BF$_4$] resonances. Asterisks (*) indicate an overlap with a resonance from the complex.

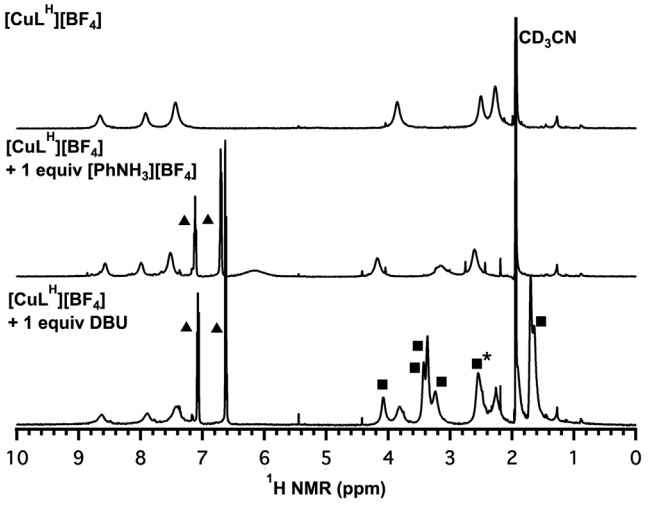

Figure 5. ^{1}H NMR of [CuL^{H}][BF$_4$] (**3**) in the presence of acid and base. Top: complex with no acid or base present. Middle: 1 equiv [PhNH$_3$][BF$_4$] added, triangle symbol (▲) indicates aniline resonances. Bottom: 1 equiv DBU added, square symbol (n) indicates [HDBU][BF$_4$] resonances. Asterisks (*) indicate an overlap with a resonance from the complex.

of one equivalent of [PhNH$_3$][BF$_4$] (pK_a = 10.62) [77] to [CuL^{DMA}][BF$_4$] (**4**) in CD$_3$CN resulted in new resonances that correspond with aniline and no resonances that correspond with anilinium, indicating complete proton transfer. No resonances consistent with free ligand were observed. The protonation is cleanly reversible; addition of one equivalent of the strong base DBU (1,8-diazabicyclo[5.4.0] undec-7-ene, pK_a = 24.34 in CH$_3$CN) [77] regenerated the initial copper complex as well as protonated DBU.

In the ^{1}H NMR spectrum of the singly protonated [CuL^{DMA}][BF$_4$] (**4**), a broad peak at 4.25 ppm resolved when the temperature was lowered to 238 K, which we assign to the proton transferred from anilinium. The ethylene diamine resonances on the complex were shifted downfield, with the methylene protons adjacent to the pyridine shifting downfield by the largest amount (0.32 ppm), followed by the methylene

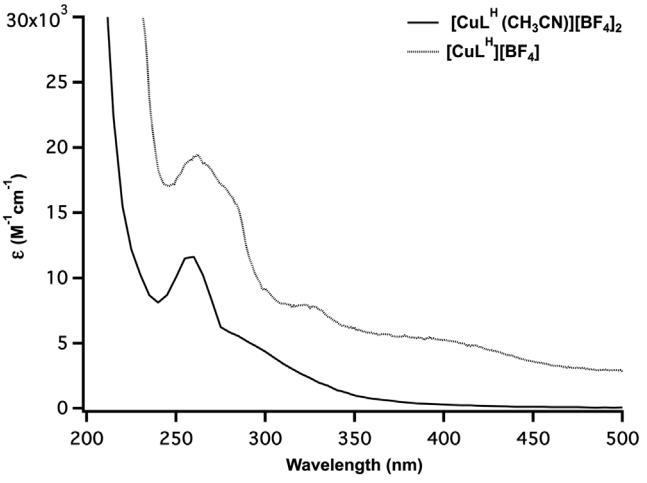

Figure 6. UV–vis spectra of $[CuL^{H}][BF_4]_2$ (**1**) (black) and $[CuL^{H}][BF_4]$ (**3**) (grey), 10 μM CH_3CN solutions.

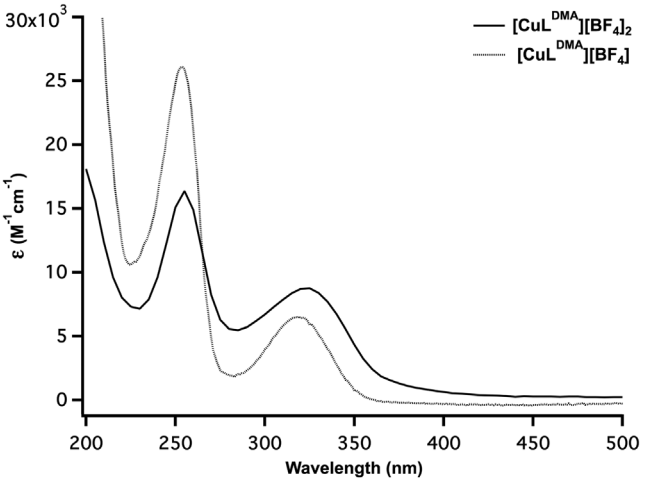

Figure 7. UV–vis spectra of $[CuL^{DMA}][BF_4]_2$ (**2**) (black) and $[CuL^{DMA}][BF_4]$ (**4**) (grey), 10 μM CH_3CN solutions.

protons in the ethyl backbone shifting downfield (0.20 ppm) and the methyl resonances on the nitrogen of the amine backbone shifting downfield (0.06 ppm). In contrast, the methyl resonances corresponding to the pendant bases only shift upfield by 0.01 ppm. This indicated protonation occurred on the tertiary amine in the ethylenediamine backbone instead of the pendant base. Variable temperature ^1H NMR spectroscopy experiments on the protonated complex (shown in Figure S6 in the Supporting Information) indicated the methylene protons in the ethyl backbone and methyl resonances on the nitrogen of the amine backbone shift upfield as the temperature is lowered. These experiments suggested protonation occurs on the ethylene diamine ligand backbone, as opposed to the pendant bases.

In order to confirm the protonation location, the same ^1H NMR spectroscopic study was performed on $[CuL^{H}][BF_4]$ (**3**), shown in Figure 5. Addition of one equivalent of $[PhNH_3][BF_4]$ in CD_3CN resulted in a similar downfield shift of the ethylene diamine resonances, with the methylene protons in the ethyl backbone shifting downfield by the largest amount (0.66 ppm), followed by the methyl resonances on the nitrogen of the amine backbone (0.34 ppm) and the methylene protons adjacent to the pyridine shifting downfield (0.31 ppm). We assign a broad resonance at 6.21 ppm to the protonated amine on

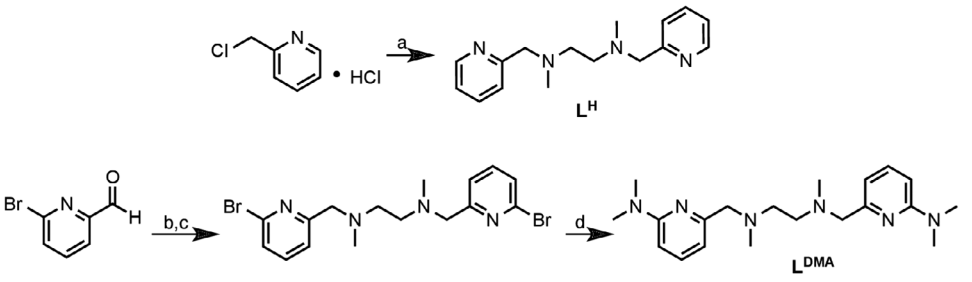

Scheme 1. Synthesis of $\mathbf{L^H}$ and $\mathbf{L^{DMA}}$. (a) N,N′-dimethylethylenediamine, TEA, (b) N,N′-dimethylethylenediamine, $NaBH(OAc)_3$, (c) NaH (d) $HN(CH_3)_2$ (40% aq).

the complex. These changes are consistent with those observed with $[CuL^{DMA}][BF_4]$ (**4**), confirming our assignment of the protonation location.

Infrared spectra of the protonated compounds of $[CuL^H][BF_4]$ (**3**) and $[CuL^{DMA}][BF_4]$ (**4**) were taken as an evaporated thin film on an Attenuated Total Reflectance (ATR) crystal. Both protonated complexes exhibited a broad absorbance around 3120 cm^{-1}, which we assign to the N-H vibration, shown in Figure S8 in the Supporting Information. This also denotes that protonation on both compounds occurs at the same location on the ligand backbone.

We were surprised that the amines on the ligand backbone are more basic than the pendant amines. However, it is worth noting that the pK_a of protonated dimethylaniline in acetonitrile is 11.43 [78] while the pK_a of protonated trialkylated amines range from 18 to 20 (protonated triethylamine is 18.82 [78], and singly protonated N,N′-dimethylethylenediamine is 19.63) [79]. From these examples, the protonated amines in the ligand backbone are estimated to be ~7 pK_a units higher than the protonated pendant bases in the free ligand. Although ligation to copper will reduce the basicity of the bound amine, protonation likely results in loss of coordination of the ethylenediamine nitrogens. The reversibility of the protonation event indicates that the amines re-coordinate upon deprotonation.

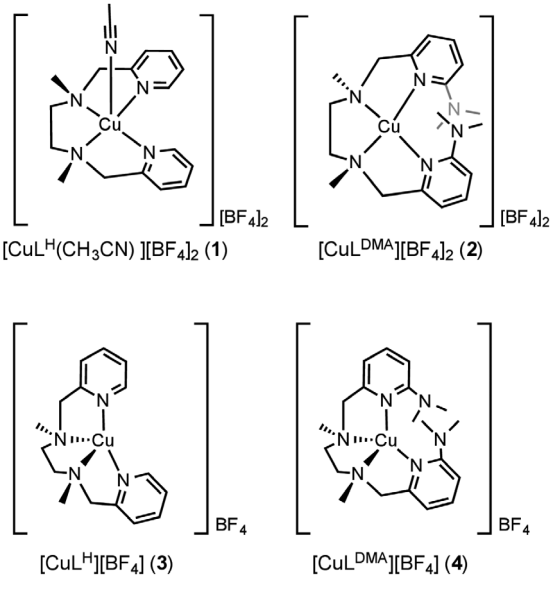

Chart 1.

2.5. Ultraviolet-visible spectra

UV–vis spectra of all complexes were taken in CH_3CN solutions. A maximum wavelength of 260 nm is observed for both $[CuL^H][BF_4]_2$ (**1**) and $[CuL^H][BF_4]$ (**3**) showing minimal change with reduction of the metal center other than the molar absorptivity (ε = 19,245 and 11,622 L (cm × mol)$^{-1}$, respectively), shown in Figure 6. The ε and its weak dependence on the metal oxidation state indicate the absorption is primarily due to π–π* transitions within the ligand.

Two absorption band maxima are seen for both $[CuL^{DMA}][BF_4]_2$ (**2**) (255 and 325 nm) and $[CuL^{DMA}][BF_4]$ (**4**) (254 and 319 nm), shown in Figure 7. Upon reduction of the metal center, the 255 nm absorption does not shift but increases in molar absorptivity (ε = 16,372 and 26,076 L (cm × mol)$^{-1}$, respectively), again indicating primarily π–π* transitions within the ligand. However, there is a hypsochromic shift from 325 to 319 nm upon one electron reduction of the metal center as well as a decrease in molar absorptivity (ε = 8767 and 6526 L (cm × mol)$^{-1}$, respectively).

3. Conclusion

We have developed an improved synthetic route to a versatile N_2Py_2 ligand with two dimethylamine functionalities in the secondary coordination sphere. Our protonation studies on the diamagnetic Cu(I) complexes of the N_2Py_2 ligands indicate that the amines located on the ligand backbone are more basic than the uncoordinated dimethylamine groups. Protonation at this site is cleanly reversible, indicating that it can serve as a proton reservoir for substrate reactivity at the metal center.

This type of protonation study using diamagnetic complexes may prove useful for other systems that incorporate pendant bases in the secondary coordination sphere. Although the pendant bases for these complexes are not as basic as we anticipated, they are still positioned to serve as hydrogen-bond acceptors to activate polar molecules bound to the metal. We are currently studying this effect with metals that prefer an octahedral geometry, since these will leave open coordination sites for substrate binding. Additionally, modifications to the ligand backbone and pendant base to adjust their respective pK_a values are ongoing.

4. Experimental

4.1. General experimental details

All reagents were purchased from commercial suppliers and used without purification. Unless otherwise noted, all organic chemical manipulations were performed in air. Compounds were purified via flash column chromatography using Sorbent Technologies 60 Å, 230–400 mesh silica gel, unless otherwise stated. Unless otherwise noted, inorganic metal complexations were performed in a Vacuum Atmospheres Co. drybox under a nitrogen atmosphere. $[Cu(CH_3CN)_4][BF_4]_2$ [80] and *N*^{1},*N*^{2}-dimethyl-*N*^{1},*N*^{2}-bis(pyridin-2-ylmethyl)ethane-1,2-diamine (**L^H**) [71] were prepared using literature methods. Anhydrous solvents were sparged with UHP argon (Praxair) and passed through columns containing Q-5 and molecular sieves before use.

^{1}H NMR spectra were recorded at 500 MHz on Bruker instruments. ^{1}H NMR spectra chemical shifts are reported as δ values in ppm relative to residual protio solvent: $CDCl_3$ (7.26 ppm), CD_3CN (1.94 ppm). Proton NMR data are reported as follows: chemical shift (δ ppm), multiplicity (s = singlet, d = doublet, t = triplet, q = quartet), coupling constants (*J*) in Hertz (Hz), and integration. Multiplets (m) are reported over the range (ppm). Electrospray ionization mass spectra (ESI-MS) were obtained on a Micromass LCT and collected at the University of California-Irvine Mass Spectrometry Facility. Elemental analyses were performed on a Perkin Elmer 2400 Series II CHNS elemental analyzer. Infrared spectra were collected using a Thermo Scientific Nicolet iS5 spectrometer with an iD5 ATR attachment in a nitrogen filled glovebox. The sample was prepared by evaporating an acetonitrile solution of the compound onto an ATR crystal. Ultraviolet-visible (UV–vis) spectra were collected as 10 μM solutions in 3 mL CH_3CN in a 1 cm quartz cuvette using an Agilent Technologies Cary 60 UV–vis spectrometer.

Electrochemical experiments were performed under an atmosphere of nitrogen in a solution containing 0.1 M Bu_4NBF_4 in acetonitrile. Glassy carbon was used as the working and auxiliary electrode and a silver wire was used as a pseudoreference electrode. Ferrocene was used as an internal standard, and all potentials are referenced to the ferrocenium/ferrocene couple. Cyclic voltammetry experiments were performed with a Pine Wavedriver 10 or 20 potentiostat and Pine Aftermath software version 1.2.7359.

4.2. Synthesis and characterization of compounds

4.2.1. N^1,N^2-bis((6-bromopyridin-2-yl)methyl)-N^1,N^2-dimethylethane-1,2-diamine

A solution of sodium triacetoxyborohydride (1.5 g, 7.2 mmol) and 6-bromo-2-formylpyridine (1.1 g, 5.4 mmol) in dry dichloromethane (20 mL) was treated with *N*,*N*′-dimethylethylenediamine (0.19 mL, 0.15 g, 1.8 mmol) and the mixture was stirred at 25 °C under nitrogen for 18 h. The resulting mixture was quenched with 20 mL sat. aqueous sodium bicarbonate. The organic layer was removed and the aqueous layer was extracted 3 × 20 mL portions of ethyl acetate. The organic layers were combined, dried over $MgSO_4$, filtered and concentrated to afford a brown oil (1.2 g, 2.8 mmol). The protonated N^1,N^2-bis((6-bromopyridin-2-yl)methyl)-N^1,N^2-dimethylethane-1,2-diamine obtained above was dissolved in 20 mL dry tetrahydrofuran. Sodium hydride (60% dispersion in mineral oil, 0.24 g, 6.1 mmol) was added and the resulting solution was stirred at 25 °C under nitrogen for 24 h. The solution was concentrated to give a brown solid that was dissolved in large portions of hexane and filtered three times. Resulting filtrate was concentrated to give a light yellow oil (0.68 g, 89% yield). ^{1}H NMR ($CDCl_3$): δ = 7.50 (t, $^3J_{HH}$ = 10.0 Hz, 2H, Ar–*H*), 7.44 (d, $^3J_{HH}$ = 10.0 Hz, 2H, Ar–*H*), 7.34 (d, $^3J_{HH}$ = 10.0 Hz, 2H, Ar–*H*), 3.67 (s, 4H, Ar–C*H*$_2$–N–), 2.61 (s, 4H, –C*H*$_2$–C*H*$_2$–), 2.27 (s, 6H, –N–C*H*$_3$).

4.2.2. Improved preparation of N,N′-bis((6-(dimethylamino)pyridin-2-yl)methyl)-N,N′-dimethylethane-1,2-diamine (L^{DMA})

To N^1,N^2-bis((6-bromopyridin-2-yl)methyl)-N^1,N^2-dimethylethane-1,2-diamine (0.68 g, 1.6 mmol) in a pressure flask were added aqueous DMA (40% w/w, 2.0 mL, 1.8 g, 16 mmol) and water (5 mL). The resulting mixture was stirred and heated to 50 °C for 48 h and then cooled to room temperature. The resulting mixture was extracted with dichloromethane several times and the organic layers were combined, dried over $MgSO_4$, filtered and concentrated to give a dark brown oil (0.54 g, 95% yield). The ligand can be observed by thin-layer chromatography on a silica plate using an eluent solution of ethyl acetate/methanol/triethylamine (89 : 10 : 1). ^{1}H NMR ($CDCl_3$): δ = 7.39 (t, $^3J_{HH}$ = 10.0 Hz, 2H, Ar-*H*), 6.64 (d, $^3J_{HH}$ = 10.0 Hz, 2H, Ar–*H*), 6.38 (d, $^3J_{HH}$ = 10.0 Hz, 2H, Ar–*H*), 3.50 (s, 4H, Ar-C*H*$_2$–N–), 3.03 (s, 12H, –N–(C*H*$_3$)$_2$), 2.60 (s, 4H, –C*H*$_2$–C*H*$_2$–), 2.26 (s, 6H, –N–C*H*$_3$).

4.2.3. $[CuL^H][BF_4]_2$ (1)

Solid $[Cu(CH_3CN)_4][BF_4]_2$ (74 mg, 0.18 mmol) was added to a solution of **L^H** (51 mg, 0.18 mmol) in 5 mL of CH_3CN. The dark blue solution was stirred at 25 °C for 0.5 h then 5 mL of Et_2O was added to precipitate the complex. The supernatant was decanted and resulting crude blue oil was triturated with toluene to achieve a dark blue powder. The crude powder was redissolved in *ca.* 1 mL of CH_3CN and layered with 4 mL of THF. After 1 day at –40 °C, dark blue solid was isolated by filtration and washed with 2 × 4 mL THF (96 mg, 94% yield). ESI-MS (CH_3CN) *m*/*z*: 166.55 ($[M-L]^{+2}$). λ_{max} = 260 nm (ε = 19,245 L (mol × cm)$^{-1}$. Anal. Calcd (Found) for $C_{16}H_{22}B_2CuF_8N_4$ (%): C, 37.86 (38.25); H, 4.37 (4.48); N, 11.04 (11.83).

4.2.4. $[CuL^{DMA}][BF_4]_2$ (2)

Solid $[Cu(CH_3CN)_4][BF_4]_2$ (56 mg, 0.14 mmol) was added to a solution of **L^{DMA}** (50. mg, 0.14 mmol) in 5 mL of CH_3CN. The dark purple solution was stirred at 25 °C for 0.5 h and then 5 mL of Et_2O was added to precipitate the complex. The supernatant was decanted and resulting purple powder redissolved in *ca.* 1 mL of CH_3CN and layered with 4 mL of Et_2O. After 1 d at –40 °C, dark purple solid was isolated by filtration and washed with 2 × 4 mL Et_2O (68 mg, 82% yield). ESI-MS (CH_3CN) *m*/*z*: 209.6 ($[M-L]^{+2}$).

λ_{max} = 255 nm (ε = 16,372 L (mol × cm)$^{-1}$) and 325 nm (ε = 8767 L (mol × cm)$^{-1}$). Anal. Calcd (Found) for $C_{20}H_{32}B_2CuF_8N_6$ (%): C, 40.46 (40.04); H, 5.43 (5.38); N, 14.16 (13.92).

4.2.5. [CuL^{H}][BF$_4$] (3)

A dark blue solution of **1** (11 mg, 19 µmol) in 3 mL of CH_3CN was cooled to –40 °C in the glovebox freezer for 2 h. The cooled solution was added to a vial containing solid KC_8 (2.7 mg, 19 µmol, 1 equiv), resulting in an immediate color change to light yellow. After stirring at room temperature for 0.5 h, the solution was filtered. Removal of solvent from the filtrate provided **3** as a light yellow powder (5.0 mg, 60% yield). ^{1}H NMR (CD_3CN) δ (ppm): 8.67 (d, $^3J_{HH}$ = 10.0 Hz, 2H, Ar–*H*), 7.93 (t, $^3J_{HH}$ = 10.0 Hz, 2H, Ar–*H*), 7.45 (m, 4H, Ar-*H*), 3.87 (s, 4H, Ar–C*H*$_2$–N–), 2.50 (s, 4H, –C*H*$_2$–C*H*$_2$–), 2.27 (s, 6H, –N–C*H*$_3$). ESI-MS (CH_3CN) *m/z*: 333.07 ([M-L]$^+$). λ_{max} = 260 nm (ε = 11,622 L (mol × cm)$^{-1}$). Anal. Calcd (Found) for $C_{16}H_{22}BCuF_4N_4$ + 1.5 CH_3CN (%): C, 47.32 (47.12); H, 5.54 (5.24); N, 15.97 (15.64).

4.2.6. [CuL^{DMA}][BF$_4$] (4)

A dark purple solution of **2** (10 mg, 17 µmol) in 3 mL of CH_3CN was cooled to -40 °C in the glovebox freezer for 2 h. The cooled solution was added to a vial containing solid KC_8 (2.3 mg, 17 µmol, 1 equiv), resulting in an immediate color change to light yellow. After stirring at room temperature for 0.5 h, the solution was filtered. Removal of solvent from the filtrate provided **4** as a light yellow powder (8.6 mg, 86% yield). ^{1}H NMR (CD_3CN) δ (ppm): 7.57 (t, $^3J_{HH}$ = 10.0 Hz, 2H, Ar–*H*), 6.75 (d, $^3J_{HH}$ = 10.0 Hz, 2H, Ar–*H*), 6.64 (d, $^3J_{HH}$ = 10.0 Hz, 2H, Ar–*H*), 3.54 (s, 4H, Ar–C*H*$_2$–N–), 3.03 (s, 12H, –N–(C*H*$_3$)$_2$), 2.79 (s, 4H, –C*H*$_2$–C*H*$_2$–), 2.37 (s, 6H, –N–C*H*$_3$). ESI-MS (CH_3CN) *m/z*: 419.15 ([M – L]$^+$). λ_{max} = 254 nm (ε = 26,076 L (mol × cm)$^{-1}$) and 319 nm (ε = 6526 L (mol × cm)$^{-1}$). Anal. Calcd (Found) for $C_{20}H_{32}BCuF_4N_6$ (%): C, 47.39 (47.73); H, 6.36 (6.35); N, 16.58 (16.07).

Supplementary material

Electronic Supplementary Information (ESI) available: CIF files (CCDC deposition numbers) for **1** (1402126), **2** (1402125), **3** (1422926), **4** (1402124), ^{1}H NMR Spectra, Cyclic Voltammetry, X-Ray Crystallographic Data Tables.

Disclosure statement

No potential conflict of interest was reported by the authors.

Funding

This work was supported by the U.S. Department of Energy, Office of Science, Office of Basic Energy Sciences [grant number DE-SC0012150].

References

[1] A. Migliore, N.F. Polizzi, M.J. Therien, D.N. Beratan. *Chem. Rev.*, **114**, 3381 (2014).
[2] S.Y. Reece, D.G. Nocera. *Annu. Rev. Biochem.*, **78**, 673 (2009).
[3] C. Tard, C.J. Pickett. *Chem. Rev.*, **109**, 2245 (2009).
[4] A. Sigel, H. Sigel, R.K.O. Sigel. *Metal Ions in Life Sciences*, John Wiley & Sons Ltd., Chichester (2006).
[5] K.B. Schowen, H.H. Limbach, G.S. Denisov, R.L. Schowen. *Biochim. Biophys. Acta, Bioenerg.*, **1458**, 43 (2000).
[6] B.S. Hammes, V.G. Young Jr., A.S. Borovik. *Angew. Chem. Int. Ed.*, **38**, 666 (1999).
[7] Z. Shirin, B.S. Hammes, V.G. Young, A.S. Borovik. *J. Am. Chem. Soc.*, **122**, 1836 (2000).
[8] C.-Y. Yeh, C.J. Chang, D.G. Nocera. *J. Am. Chem. Soc.*, **123**, 1513 (2001).
[9] C.E. MacBeth, P.L. Larsen, T.N. Sorrell, D. Powell, A.S. Borovik. *Inorg. Chim. Acta*, **341**, 77 (2002).
[10] A.S. Borovik. *Acc. Chem. Res.*, **38**, 54 (2005).
[11] P.J. Zinn, D.R. Powell, V.W. Day, M.P. Hendrich, T.N. Sorrell, A.S. Borovik. *Inorg. Chem.*, **45**, 3484 (2006).
[12] J.Y. Yang, J. Bachmann, D.G. Nocera. *J. Org. Chem.*, **71**, 8706 (2006).
[13] J.Y. Yang, S.Y. Liu, I.V. Korendovych, E.V. Rybak-Akimova, D.G. Nocera. *ChemSusChem*, **1**, 941 (2008).
[14] J.Y. Yang, D.G. Nocera. *Tetrahedron Lett.*, **49**, 4796 (2008).

[15] A.J. Kendall, L.N. Zakharov, J.D. Gilbertson. *Inorg. Chem.*, **49**, 8656 (2010).
[16] J.L. Boyer, D.E. Polyansky, D.J. Szalda, R. Zong, R.P. Thummel, E. Fujita. *Angew. Chem.*, **123**, 12808 (2011).
[17] L.E. Cheruzel, J. Cui, M.S. Mashuta, C.A. Grapperhaus, R.M. Buchanan. *Tetrahedron Lett.*, **52**, 4771 (2011).
[18] C.M. Moore, N.K. Szymczak. *Dalton Trans.*, **41**, 7886 (2012).
[19] J.S. Hart, G.S. Nichol, J.B. Love. *Dalton Trans.*, **41**, 5785 (2012).
[20] C.M. Moore, N.K. Szymczak. *Chem. Commun.*, **49**, 400 (2013).
[21] O. Tutusaus, C. Ni, N.K. Szymczak. *J. Am. Chem. Soc.*, **135**, 3403 (2013).
[22] T.S. Teets, J.A. Labinger, J.E. Bercaw. *Organometallics*, **32**, 5530 (2013).
[23] E.M. Matson, Z. Gordon, B. Lin, M.J. Nilges, A.R. Fout. *Dalton Trans.*, **43**, 16992 (2014).
[24] E.M. Matson, J.A. Bertke, A.R. Fout. *Inorg. Chem.*, **53**, 4450 (2014).
[25] J.V. Gavette, C.M. Klug, L.N. Zakharov, M.P. Shores, M.M. Haley, D.W. Johnson. *Chem. Commun.*, **50**, 7173 (2014).
[26] S. Bosch, P. Comba, L.R. Gahan, G. Schenk. *Inorg. Chem.*, **53**, 9036 (2014).
[27] M. Adelhardt, M.J. Chalkley, F.W. Heinemann, J. Sutter, A. Scheurer, K. Meyer. *Inorg. Chem.*, **53**, 2763 (2014).
[28] W.A. Hoffert, M.T. Mock, A.M. Appel, J.Y. Yang. *Eur. J. Inorg. Chem.*, **2013**, 3846 (2013).
[29] J.J. Warren, J.M. Mayer. *Biochemistry*, **54**, 1863 (2015).
[30] C.M. Moore, N.K. Szymczak. *Chem. Sci.*, **6**, 3373 (2015).
[31] C.J. Weiss, E.S. Wiedner, J.A.S. Roberts, A.M. Appel. *Chem. Commun.*, **51**, 6172 (2015).
[32] S.T. Ahn, E.A. Bielinski, E.M. Lane, Y. Chen, W.H. Bernskoetter, N. Hazari, G.T.R. Palmore. *Chem. Commun.*, **51**, 5947 (2015).
[33] P. Das, M.-H. Ho, M. O'Hagan, W.J. Shaw, R. Morris Bullock, S. Raugei, M.L. Helm. *Dalton Trans.*, **43**, 2744 (2014).
[34] C. Costentin, G. Passard, M. Robert, J.-M. Savéant. *J. Am. Chem. Soc.*, **136**, 11821 (2014).
[35] C.J. Weiss, P. Das, D.L. Miller, M.L. Helm, A.M. Appel. *ACS Catalysis*, **4**, 2951 (2014).
[36] R.M. Bullock, A.M. Appel, M.L. Helm. *Chem. Commun.*, **50**, 3125 (2014).
[37] B.H. Solis, S. Hammes-Schiffer. *Inorg. Chem.*, **53**, 6427 (2014).
[38] E.M. Matson, Y.J. Park, A.R. Fout. *J. Am. Chem. Soc.*, **136**, 17398 (2014).
[39] B.D. Matson, C.T. Carver, A. Von Ruden, J.Y. Yang, S. Raugei, J.M. Mayer. *Chem. Commun.*, **48**, 11100 (2012).
[40] C. Costentin, S. Drouet, M. Robert, J.-M. Saveant. *Science*, **338**, 90 (2012).
[41] C.T. Carver, B.D. Matson, J.M. Mayer. *J. Am. Chem. Soc.*, **134**, 5444 (2012).
[42] C.S. Seu, A.M. Appel, M.D. Doud, D.L. DuBois, C.P. Kubiak. *Energy Environ. Sci.*, **5**, 6480 (2012).
[43] J.Y. Yang, R.M. Bullock, M.R. DuBois, D.L. DuBois. *MRS Bulletin*, **36**, 39 (2011).
[44] R.L. Shook, S.M. Peterson, J. Greaves, C. Moore, A.L. Rheingold, A.S. Borovik. *J. Am. Chem. Soc.*, **133**, 5810 (2011).
[45] B.R. Galan, J. Schöffel, J.C. Linehan, C. Seu, A.M. Appel, J.A.S. Roberts, M.L. Helm, U.J. Kilgore, J.Y. Yang, D.L. DuBois, C.P. Kubiak. *J. Am. Chem. Soc.*, **133**, 12767 (2011).
[46] D.K. Dogutan, R. McGuire, D.G. Nocera. *J. Am. Chem. Soc.*, **133**, 9178 (2011).
[47] D.K. Dogutan, S.A. Stoian, R. McGuire, M. Schwalbe, T.S. Teets, D.G. Nocera. *J. Am. Chem. Soc.*, **133**, 131 (2011).
[48] J.Y. Yang, R.M. Bullock, W.G. Dougherty, W.S. Kassel, B. Twamley, D.L. DuBois, M. Rakowski DuBois. *Dalton Trans.*, **39**, 3001 (2010).
[49] R. McGuire Jr., D.K. Dogutan, T.S. Teets, J. Suntivich, Y. Shao-Horn, D.G. Nocera. *Chem. Sci.*, **1**, 411 (2010).
[50] M. Rakowski Dubois, D.L. Dubois. *Acc. Chem. Res.*, **42**, 1974 (2009).
[51] G.M. Jacobsen, J.Y. Yang, B. Twamley, A.D. Wilson, R.M. Bullock, M. Rakowski, D.L. DuBois. *Energy Environ. Sci.*, **1**, 167 (2008).
[52] J.Y. Yang, D.G. Nocera. *J. Am. Chem. Soc.*, **129**, 8192 (2007).
[53] M.C. White, A.G. Doyle, E.N. Jacobsen. *J. Am. Chem. Soc.*, **123**, 7194 (2001).
[54] A. Murphy, A. Pace, T.D.P. Stack. *Org. Lett.*, **6**, 3119 (2004).
[55] S. Taktak, S.V. Kryatov, T.E. Haas, E.V. Rybak-Akimova. *J. Mol. Catal. A: Chem.*, **259**, 24 (2006).
[56] O.Y. Lyakin, K.P. Bryliakov, E.P. Talsi. *Inorg. Chem.*, **50**, 5526 (2011).
[57] L.S. Morris, M.P. Girouard, M.H. Everhart, W.E. McClain, J.A. van Paridon, R.D. Pike, C. Goh. *Inorg. Chim. Acta*, **413**, 149 (2014).
[58] S. McArthur, M.C. Baird. *Eur. Polym. J.*, **55**, 170 (2014).
[59] D. Tetard, J.-B. Verlhac. *J. Mol. Catal. A: Chem.*, **113**, 223 (1996).
[60] G.J.P. Britovsek, J. England, A.J.P. White. *Inorg. Chem.*, **44**, 8125 (2005).
[61] E.A. Turitsyna, O.N. Gritsenko, A.A. Shteinman. *Kinet. Catal.*, **48**, 53 (2007).
[62] O.V. Makhlynets, E.V. Rybak-Akimova. *Chem. – A Eur. J.*, **16**, 13995 (2010).
[63] Y. He, J.D. Gorden, C.R. Goldsmith. *Inorg. Chem.*, **50**, 12651 (2011).
[64] Q. Zhang, J.D. Gorden, C.R. Goldsmith. *Inorg. Chem.*, **52**, 13546 (2013).
[65] A. Kejriwal, A. Biswas, A. Choudhury, P. Bandyopadhyay. *Transition Met. Chem.*, **39**, 909 (2014).
[66] C.-K. Li, W.-T. Tang, C.-M. Che, K.-Y. Wong, R.-J. Wang, T.C.W. Mak. *J. Chem. Soc., Dalton Trans.*, 1909 (1991).
[67] J.L. Fillol, Z. Codolà, I. Garcia-Bosch, L. Gómez, J.J. Pla, M. Costas. *Nat. Chem.*, **3**, 807 (2011).
[68] R.M. Henry, R.K. Shoemaker, D.L. DuBois, M.R. DuBois. *J. Am. Chem. Soc.*, **128**, 3002 (2006).
[69] G.M. Jacobsen, R.K. Shoemaker, M. Rakowski DuBois, D.L. DuBois. *Organometallics*, **26**, 4964 (2007).
[70] M. Delgado, S.K. Sommer, S.P. Swanson, R.F. Berger, T. Seda, L.N. Zakharov, J.D. Gilbertson. *Inorg. Chem.*, **54**, 7239 (2015).
[71] F.A. Mautner, M. Koikawa, M. Mikuriya, E.V. Harrelson, S.S. Massoud. *Polyhedron*, **59**, 17 (2013).

[72] I. Tsukamoto, H. Koshio, T. Kuramochi, C. Saitoh, H. Yanai-Inamura, C. Kitada-Nozawa, E. Yamamoto, T. Yatsu, Y. Shimada, S. Sakamoto, S.-I. Tsukamoto. *Bioorg. Med. Chem.*, **17**, 3130 (2009).
[73] D. Maiti, A.A. Narducci Sarjeant, K.D. Karlin. *J. Am. Chem. Soc.*, **129**, 6720 (2007).
[74] A.W. Addison, T.N. Rao, J. Reedijk, J. van Rijn, G.C. Verschoor. *J. Chem. Soc., Dalton Trans.*, 1349 (1984).
[75] L. Yang, D.R. Powell, R.P. Houser. *Dalton Trans.*, 955 (2007).
[76] M. Hirotsu, N. Kuwamura, I. Kinoshita, M. Kojima, Y. Yoshikawa, K. Ueno. *Dalton Trans.*, 7678 (2009).
[77] I. Kaljurand, A. Kütt, L. Sooväli, T. Rodima, V. Mäemets, I. Leito, I.A. Koppel. *J. Org. Chem.*, **70**, 1019 (2005).
[78] I. Kaljurand, T. Rodima, I. Leito, I.A. Koppel, R. Schwesinger. *J. Org. Chem.*, **65**, 6202 (2000).
[79] E.-I. Rõõm, A. Kütt, I. Kaljurand, I. Koppel, I. Leito, I.A. Koppel, M. Mishima, K. Goto, Y. Miyahara. *Chem. – A Eur. J.*, **13**, 7631 (2007).
[80] D. Coucouvanis, *Inorganic Syntheses*, New York, John Wiley & Sons, Inc. Vol. 33, pp. 75–121 (2002).